HHS Public Access

Author manuscript

Nat Cell Biol. Author manuscript; available in PMC 2019 October 15.

Published in final edited form as:

Nat Cell Biol. 2019 May ; 21(5): 560–567. doi:10.1038/s41556-019-0308-3.

Engineering a haematopoietic stem cell niche by revitalizing mesenchymal stromal cells

Fumio Nakahara[1,2,6], **Daniel K. Borger**[1,2], **Qiaozhi Wei**[1,2], **Sandra Pinho**[1,2,5], **Maria Maryanovich**[1,2], **Ali H. Zahalka**[1,2], **Masako Suzuki**[3], **Cristian D. Cruz**[1,2], **Zichen Wang**[4], **Chunliang Xu**[1,2], **Philip E. Boulais**[1,2], **Avi Ma'ayan**[4], **John M. Greally**[3,5], and **Paul S. Frenette**[1,2,5]

[1]Ruth L. and David S. Gottesman Institute for Stem Cell and Regenerative Medicine Research, Albert Einstein College of Medicine, Bronx, NY 10461, USA

[2]Department of Cell Biology, Albert Einstein College of Medicine, Bronx, New York, USA

[3]Center for Epigenomics, Department of Genetics, Albert Einstein College of Medicine, Bronx, New York, USA

[4]Department of Pharmacological Sciences, Mount Sinai Center for Bioinformatics, Icahn School of Medicine at Mount Sinai, New York, NY 10029, USA

[5]Department of Medicine, Albert Einstein College of Medicine, Bronx, New York, USA

[6]Present address: Department of Hematology and Oncology, Graduate School of Medicine, The University of Tokyo, Tokyo 113-8655, Japan (F.N.)

Abstract

Haematopoietic stem cells (HSCs) are maintained by bone marrow (BM) niches *in vivo*[1,2], but the ability of niche cells to maintain HSCs *ex vivo* is markedly diminished. Expression of niche factors by Nestin-GFP$^+$ mesenchymal-derived stromal cells (MSCs) is downregulated upon culture, suggesting that transcriptional rewiring may contribute to this reduced HSC maintenance potential. Using an RNA sequencing screen, we identified 5 transcription factors (*Klf7*, *Ostf1*,

Correspondence and requests for materials should be addressed to P.S.F. (paul.frenette@einstein.yu.edu).

Author Contributions

F.N. designed the study, performed most of the experiments and analysed data. D.K.B. performed *Mef2c* and *Klf7* overexpression experiments, helped with co-culture experiments, and analysed data. Q.W. advised on experiment design and helped with making the list of candidate genes from RNA-seq data. S.P. advised on experiment design and helped with implantation experiments of hydroxyapatite scaffolds. M.M. advised on experiment design and helped with HSC imaging. A.H.Z. advised on experiment design. M.S. and J.M.G. analysed the ATAC-seq data. C.D.C. helped with vector cloning and virus production. Z.W. and A.M. analysed the RNA-seq data. P.E.B and C.X. helped with improving culture system. P.S.F. supervised the study. F.N. and P.S.F. interpreted data and wrote the manuscript. All authors discussed the results and commented on the manuscript.

The authors declare no competing financial interests.

Code Availability

All code used in this study are available from the corresponding author upon reasonable request

Data Availability

RNA-seq and ATAC-seq data have been deposited in Gene Expression Omnibus, accession number GSE112233. Source data for Fig. 1–4 and Supplementary Fig. 1–4 have been provided as Supplementary Table 6. All other data supporting the findings of this study are available from the corresponding author upon reasonable request.

Xbp1, *Irf3*, *Irf7*) that restored HSC niche function in cultured BM-derived MSCs. These revitalized MSCs (rMSCs) exhibited enhanced synthesis of HSC niche factors while retaining their mesenchymal differentiation capacity. In contrast to HSCs co-cultured with control MSCs, HSCs expanded with rMSCs showed higher repopulation capacity and protected lethally irradiated recipient mice. Competitive reconstitution assays revealed ~7-fold expansion of functional HSCs by rMSCs. rMSCs prevented the accumulation of DNA damage in cultured HSCs, a hallmark of ageing and replication stress. Analysis of the reprogramming mechanisms uncovered a role for myocyte enhancer factor 2c (*Mef2c*) in the revitalization of MSCs. These results provide insight in the transcriptional regulation of the niche with implications for stem cell-based therapies.

HSCs are notoriously difficult to maintain in culture, possibly due to our limited understanding of the microenvironment that sustains them *in vivo*. Although BM perivascular stromal cells (e.g. those marked by Nestin-GFP) express high levels of niche factors[3–5], their ability to maintain HSCs *ex vivo* is modest compared to BM-derived endothelial cells[6–8]. We compared the expression levels of selected HSC niche genes (*Scf*, *Cxcl12*, *Vcam1* and *Angpt1*) in freshly isolated Nestin-GFP$^+$ or Nestin-GFP$^-$ fractions of BM CD45$^-$Ter119$^-$CD31$^-$ cells, against Nestin-GFP$^+$ cells cultured for 2 weeks in CFU-F culture media (designed to maintain MSC multipotency). The expression of HSC niche factors was highly enriched in Nestin-GFP$^+$ cells compared to the Nestin-GFP$^-$ cell fraction, but the expression of these genes was dramatically reduced upon culture (Fig.1a). We hypothesized that the impaired niche function might result from alterations in the transcriptional machinery following the removal of niche cells from their natural environment.

While roles for a handful of transcription factors in BM development have been described previously[9–11], the transcriptional network specifying the HSC niche remains largely unresolved. To gain further insight, we searched RNA sequencing data[12] for transcriptional regulators that were highly expressed in Nestin-GFP$^+$ stroma, revealing 40 potential candidates (Fig.1b). We compared the expression of these genes by real-time quantitative PCR (qPCR) in freshly isolated Nestin-GFP$^+$ or Nestin-GFP$^-$ BM CD45$^-$Ter119$^-$CD31$^-$ cells, with that of cultured Nestin-GFP$^+$ stroma. The ideal candidate genes were predicted to be selectively expressed in fresh Nestin-GFP$^+$ stroma, but downregulated after culture. These analyses yielded 28 genes (Fig.1c, **upper and middle panels**) after the elimination of 12 candidates due to non-specific expression or lack of downregulation after culture (Fig.1c, **lower panel**). We cultured stromal cells isolated from *Scf*-GFP knock-in mice in which GFP expression reflects endogenous *Scf* mRNA synthesis[13]. Upon culture, GFP expression was rapidly downregulated in these cells, demonstrating the potential of using GFP to screen for factors capable of revitalizing niche activity (Fig.1d). We generated lentiviral vectors expressing 28 selected genes and transduced the viral mixture into stromal cell cultures derived from *Scf*-GFP mice. Five days after transduction, we observed re-emergence of GFP$^+$ cells (Fig.1d). These GFP$^+$ cells were sorted and plated in limiting dilutions to isolate single cell-derived clones. Using this approach, we generated 16 independent GFP$^+$ single cell-derived clones in which virally integrated genes were identified by PCR (Fig.1d). We found that 4 genes [Osteoclast-stimulating factor-1 (*Ostf1)*, X-box binding protein-1 (*Xbp1)*, Interferon regulatory factor-3 (*Irf3)* and Interferon regulatory factor-7 (*Irf7)*] were virally

integrated in >75% of the clones (Fig.2a). We confirmed that all 28 genes were integrated in the bulk fraction of transduced cells (without sorting *Scf*-GFP$^+$ cells) 5 days post-transduction, while no integrated gene was detected in the bulk fraction transduced with control lentivirus containing an empty vector (Fig.2b), confirming that the lentiviruses harbouring 28 selected genes were all functional.

We next evaluated the expression levels of niche factors in the 16 single cell-derived clones and empty vector-transduced control stroma. While the expression of *Scf*, *Cxcl12*, *Vcam1* and *Angpt1* is tightly correlated upon HSC maintenance[14], their expression was variable among the clones and only clone C5 exhibited significant elevations of all niche genes (Fig. 2c and Supplementary Fig.1a–c). To assess the niche-revitalizing requirement of each of the 4 transcription regulators, we sequentially omitted each gene from the transduction cocktail. Remarkably, all 4 factors (*Ostf1*, *Xbp1*, *Irf3* and *Irf7*, or "OXII") were required for the re-appearance and expansion of Scf-GFP$^+$ cells in culture (Supplementary Fig.1d). To determine the specific combination of genes that enabled cultured stromal cells to regain their capacity to maintain and expand HSCs *in vitro*, lineage-negative (Lin$^-$) BM cells were co-cultured with each single cell-derived clone or control stroma in the presence of SCF (20 ng/ml) and TPO (10 ng/ml). After 6 days of co-culture, the number of phenotypic Lin$^-$Sca1$^+$c-Kit$^+$ (LSK) CD150$^+$CD48$^-$ HSCs was assessed by FACS. Clone C5, which has five integrated and actively expressed genes [Kruppel-like factor-7 (*Klf7*), *Ostf1*, *Xbp1*, *Irf3* and *Irf7*] (Supplementary Fig.1e–i), expanded HSCs more efficiently than any of the other clones analysed (> 4-fold compared to control stroma; Fig.2d). We compared the HSC niche capacity of newly generated single cell-derived clones using the combination of 4 factors (OXII) or 5 factors from clone C5 (*Klf7*, *Ostf1*, *Xbp1*, *Irf3* and *Irf7*, or "KOXII"). KOXII-integrated clones exhibited increased expression of niche genes compared to OXII-integrated clones (Fig.2e, Supplementary Fig.1j and 1k). Overexpression of *Klf7* alone did not similarly increase expression of *Scf* or *Cxcl12* (Supplementary Fig.1l and 1m). To test the HSC expansion function of OXII- and KOXII-integrated clones, Lin$^-$ BM cells were co-cultured with stromal cells derived from either set of clones. FACS analyses revealed a greater HSC expansion (1.7-fold) on KOXII clones compared to the OXII clones (Fig.2f). The addition of *Klf7* to the transduction cocktail (OXII) also increased the re-appearance and expansion of *Scf*-GFP$^+$ stromal cells (Supplementary Fig.1d). Altogether these results indicate that the combination of 5 genes (KOXII) reprograms cultured stromal cells into revitalized niche cells that exhibit increased expression of niche factors and improved capacity to expand phenotypic HSCs *in vitro*.

As niche activity has been shown to correlate with adult MSC activity characterized by colony-forming capacity and ability to differentiate into bone, cartilage and adipocytes[5,8], we tested the MSC activity of KOXII-integrated stromal cells (hereafter referred to as revitalized MSCs or rMSCs). rMSCs homogeneously expressed the MSC markers PDGFRα and CD51[8] (94.8 ± 2.5%) in contrast to control stromal cells (53.7 ± 3.5%; Supplementary Fig.2a). Other MSC markers, such as CD105 and LepR, were also upregulated in rMSCs compared to control MSCs, while CD44 and Sca-1 were highly expressed in both rMSCs and control MSCs (Supplementary Fig.2b). rMSCs exhibited large nuclei with prominent chromatin, which is characteristic of MSC morphology (Fig.2g). rMSCs exhibited greater mesensphere-forming activity and generated larger mesenspheres compared to control MSCs

(Supplementary Fig.2c and 2d), suggesting enhanced *in vitro* self-renewal and proliferation of rMSCs. In addition, clonally derived rMSCs generated the three major adult mesenchymal lineages (adipogenic, osteogenic and chondrogenic; Supplementary Fig.2e–g), although the ability of rMSCs to differentiate towards the osteogenic lineage was reduced as compared to control MSCs (Supplementary Fig.2f).

To evaluate the *in vitro* capacity of rMSCs to expand and maintain functional HSCs, we compared rMSCs with MS-5, a stromal cell line capable of maintaining haematopoiesis[15], as well as empty vector-transduced control MSCs and a group without stromal cell support. Using these conditions, rMSCs expanded HSC numbers *in vitro* in serum-free media supplemented with TPO (10 ng/ml) with or without SCF, expanding phenotypic HSCs > 2.1-fold without SCF, and > 4.3-fold when supplemented with SCF (20 ng/ml), relative to input (Fig.3a). Compared to MS-5 cells, rMSCs expanded HSCs >3.5-fold without SCF and >5.4-fold with SCF (Fig.3a). rMSCs also expanded the LSK fraction more than MS-5 or empty vector-transduced stromal cells, both with or without SCF (Supplementary Fig.3a). The expansion of the Lin^- (progenitor-enriched) fraction by rMSCs was lower compared to MS-5 cells in the absence of SCF, although this difference disappeared in the presence of SCF (Supplementary Fig.3a). To evaluate the contribution of soluble factors alone, we cultured HSCs with media conditioned by rMSCs and found that conditioned media was sufficient to expand HSCs (Supplementary Fig.3b). These results indicate that rMSCs expand HSCs and progenitors largely via soluble factors more effectively than either MS-5 or non-revitalized stroma.

We next evaluated the impact of rMSCs on HSC function. First, we assessed the ability of HSCs expanded *in vitro* on rMSCs to repopulate lethally irradiated recipient mice by competitive transplantation. We found a greater repopulation capacity in all three lineages (myeloid, B cell and T cell) of HSCs co-cultured with rMSCs compared to control vector-transduced MSCs (Fig.3b and 3c). This advantage was retained upon secondary transplantation (Fig.3d). Second, we found that the ability to protect lethally irradiated recipient mice was significantly improved when whole BM mononuclear cells (BMNCs) were expanded with rMSCs before transplantation (Fig.3e and Supplementary Fig.3c). These differences were particularly obvious when low numbers of BMNCs (25,000 cells) were used for transplantation (Fig.3e). Finally, we carried out competitive transplantation assays using limiting dilutions of fresh and BMNCs expanded for 6 days with rMSCs in serum-free media supplemented with SCF and TPO. The frequency of long-term repopulating HSCs was increased ~7-fold (from 1 in 22,908 fresh BM cells to 1 in 3,329 in rMSC-expanded cells; Fig.3f and Supplementary Fig.3d). These data demonstrate that rMSCs are capable of efficiently expanding functional HSCs.

The accumulation of DNA damage in HSCs during ageing[16–19] or as a result of replication errors during active HSC proliferation[20] can threaten genomic integrity and HSC function. We evaluated the ability of rMSCs to protect expanding HSCs from accumulating DNA damage. Lin^- BM cells were co-cultured with rMSCs, control MSCs, or in the absence of stroma, and phosphorylation of the histone variant H2AX at Ser139 (γH2AX), an early step in the canonical DNA damage response[16,17], was then assessed. Interestingly, a large fraction (>50%) of HSCs cultured in the absence of stroma or in the presence of control

MSCs developed γH2AX foci (Fig.3g and 3h). By contrast, HSCs co-cultured with rMSCs were significantly protected from acquisition of γH2AX foci (Fig.3h). This was also evident after scoring the number of γH2AX foci in each HSC (Supplementary Fig.3e). These results indicate that rMSCs mitigate DNA damage / replication stress in *in vitro*-expanded HSCs.

To determine whether murine rMSCs could expand human HSCs, we co-cultured isolated $CD34^+$ cells from human cord blood (CB) with murine rMSCs or control MSCs. After 6 days of co-culture, the number of phenotypic Lin^- $CD34^+$ $CD38^-$ $CD90^+$ $CD49f^+$ human HSCs was expanded 28-fold compared to input and was significantly higher on rMSCs compared to control MSCs (Fig.3i). We also carried out competitive transplantation assays using limiting dilutions of fresh and $CD34^+$ CB cells expanded for 6 days with murine rMSC. The frequency of long-term repopulating HSCs was increased ~6-fold (from 1 in 8,916 fresh CB cells to 1 in 1,566 in rMSC-expanded cells; Fig.3j and Supplementary Fig. 3f). These data demonstrate that murine rMSCs are capable of efficiently expanding functional human HSCs.

To evaluate the extent to which rMSCs resemble freshly isolated MSCs, we employed RNA-seq analysis to compare the transcriptome of freshly sorted *Scf*-GFP^- $CD45^-Ter119^-CD31^-$ cells, *Scf*-GFP^+ $CD45^-Ter119^-CD31^-$ cells, rMSCs and control vector-transduced stroma. HSC niche-associated genes were highly expressed in both native *Scf*-GFP^+ cells and rMSCs compared to the *Scf*-GFP^- cell fraction and cultured control MSCs. Interestingly, several niche-associated genes (e.g. *Runx2, Sp7, Bmp5* and *Ptn*) that are also known regulators of osteogenesis were not fully restored in rMSCs compared to native *Scf*-GFP^+ stroma (Fig.4a), likely explaining the reduced *in vitro* osteogenic differentiation capacity of rMSCs (Supplementary Fig.2f). Principal component analysis (PCA) revealed that the 4 populations clustered independently (Fig.4b). We next assessed the overlap of upregulated genes in rMSCs compared to cultured control MSCs (red, Fig.4c) and genes upregulated in freshly isolated native *Scf*-GFP^+ stromal cells compared to native *Scf*-GFP^- cells (green, Fig.4c). We found that 235 genes overlapped between these two groups, and pathway analysis revealed a highly significant increase in Rap1 signalling and Axon guidance pathways, and PI3K-Akt and Ras signalling which are important for cell survival and proliferation (Fig.4d). Interestingly, the enrichment analysis also showed significant upregulation of TGF-β signalling which is reported to promote HSC quiescence[21]. These data indicate that although rMSCs are reprogrammed to regain HSC niche function, they remain distinct from their endogenous counterparts.

To investigate the revitalization mechanism, we interrogated by Assay for Transposase Accessible Chromatin with high-throughput sequencing (ATAC-seq) the accessible DNA regions in our 4 studied populations. We found that revitalization of MSCs led to 9,623 peaks of open chromatin in rMSCs when compared to control MSCs (Fig.4e). Of these, 626 open peaks were also detected in freshly isolated *Scf*-GFP^+ cells when compared to *Scf*-GFP^- cells (Fig.4e; Supplementary Table 1 and 2). Pathway analysis of the genes closest to these 626 peaks showed overlapping pathways with those identified in RNA-seq analysis (Supplementary Fig.4a). Motif analyses of the sequence at these 626 peaks revealed that myocyte enhancer factor 2c (*Mef2c*) was among the most significantly enriched transcription regulators (p-value: 1×10^{-15}; Fig.4e). *Mef2c* was also expressed at high levels

in both rMSCs and freshly isolated *Scf*-GFP$^+$ cells compared to control cultured MSCs and freshly isolated *Scf*-GFP$^-$ cells by RNA-seq (Supplementary Fig.4b) and real-time qPCR (Fig.4f). To evaluate the role of *Mef2c* in rMSCs, we knocked down *Mef2c* in rMSCs by short hairpin RNA lentiviral transduction (shMef2c) (Supplementary Fig.4c). We found that the expression of niche factors (*Scf*, *Cxcl12* and *Vcam1*) was reduced in shMef2c-transduced compared to parental rMSCs (Supplementary Fig.4d). In addition, shMef2c transduced-rMSCs exhibited reduced (by 43%) capacity to expand HSCs in co-culture compared to shCntrl transduced-rMSCs (Fig.4g). Interestingly, overexpression of *Mef2c* in rMSCs also reduced their ability to expand HSCs in co-culture, suggesting that revitalization requires a careful regulation of *Mef2c* expression levels (Supplementary Fig.4e and 4f). These results suggest a role for *Mef2c* as a downstream effector mediating MSC revitalization.

Stromal cells cultured as feeder layers or in 3D scaffolds have been used to support HSCs *ex vivo*[22,23], but these culture systems largely promote the expansion of committed progenitors with the loss of multipotent HSCs. Our results indicate that rMSCs are able to expand multipotent HSCs and protect HSCs against DNA damage/replicative stress, relative to standard stromal cell or cell-free systems. The mechanisms behind this effect on DNA damage are unknown; it is likely that the revitalization of MSCs may also induce the expression of yet unidentified stromal-derived factors promoting HSC maintenance. Given the high sensitivity of HSCs to replicative stress, the maintenance of HSCs' genomic integrity will be important for the development of cell therapies[24].

Our results suggest that all five KOXII genes are necessary to fully restore the niche activity in MSCs *ex vivo*. Some of these genes may act singly, perhaps by preventing MSC differentiation[25] or driving expansion of haematopoietic growth factors[26]. In cooperation, these 5 factors enhance several key signaling pathways (e.g. TGF-β, PI3K-Akt, Ras and TNF signaling) that may contribute to revitalization. We have also identified *Mef2c* as an important transcription factor downstream of KOXII, and whose expression is restored to the levels of native niche cells. Our results thus establish a new platform that provides critical insight in the regulatory network of the HSC niche and forms the basis toward the engineering of supportive niches for curative cell therapies.

Methods

Mice

Scf-GFP knock-in mice (Kitl$^{tm1.1Sjm}$)[13] were kindly provided by L. Ding (Columbia University). *Nestin*–GFP mice[12] were bred in our facilities. C57BL/6-CD45.1/2 congenic strains were purchased from the National Cancer Institute or the Jackson laboratory. All mice were analysed at 8–12 weeks of age. All experimental procedures were approved by the Institutional Animal Care and Use Committees of Albert Einstein College of Medicine, and all research was in compliance with all relevant ethical regulations.

Sample preparation for flow cytometry and cell sorting

For the analysis of haematopoietic cells, nucleated single-cell suspensions enriched from BM were obtained by flushing and dissociating BM plugs using a 21G needle in phosphate-buffered saline (PBS; Gibco). Single-cell suspensions enriched from peripheral blood were obtained by retro-orbital bleeding of mice. For analysis of stromal cell populations, intact flushed BM plugs were digested for 30 min at 37°C in 1mg/ml Collagenase type IV (Gibco) and 2mg/ml Dispase (Gibco) in Hank's balanced salt solution (HBSS; Gibco). After lysing red blood cell (RBC) with ammonium chloride, cells were filtered through 70 μm nylon mesh. For FACS analysis or sorting, cells were stained with antibodies in PEB (PBS containing 0.5 % BSA and 2 mM EDTA). Dead cells and debris were excluded by FSC, SSC and DAPI (4', 6-diamino-2-phenylindole; Sigma) staining profiles. FACS analyses were carried out using BD LSRII flow cytometer (BD Biosciences) and cell sorting experiments were performed using BD FACSAria II Cell Sorter (BD Biosciences). Data were analysed with FlowJo 10.0.8 (LLC) or FACS Diva 6.1 software (BD Biosciences).

Flow cytometry antibodies

The following antibodies were used for flow cytometry: Anti-CD150-PE (TC15–12F12.2; 115904), anti-CD117-PE/Cy7 (2B8; 105814), anti-CD45.2-PE (104; 109807), anti-CD48-Alexa Fluor 647 (HM48–1; 103416) were purchased from BioLegend (San Diego, CA). anti-CD45-APC-eFluor 780 (30-F11; 47–0451-82), anti-Ter119-APC-eFluor 780 (TER-119; 47–5921-82), Streptavidin APC-eFluor 780 (47–4317-82), anti-CD31-PE/Cy7 (MEC13.3; 25–0311-82), anti-CD45.1-FITC (A20; 11–0453-85), anti-B220-APC-eFluor 780 (RA3–6B2; 47–0452-82), anti-CD4-PE/Cy7 (GK1.5; 25–0041-82), anti-CD8a-PE/Cy7 (53–6.7; 25–0081-85), CD51-PE (RMV-7; 13–0512-85), anti-PDGFRα (CD140a)-APC (APA5; 17–1401-81), anti-Ly6A/E(Sca-1)-FITC (D7; 11–5981-82), Anti-CD45-PerCp-Cyanine5.5 (30-F11; 45–0451-82), anti-CD11b (Mac-1)-PE (M1/70; 12–0112-83) were purchased from eBioscience (Thermo Fisher). Anti-lineage panel cocktail (TER-119, RB6–8C5, RA3–6B2, M1/70, 145–2C11 at 1:50 dilution) was from BD Biosciences (559971). Unless otherwise specified, all antibodies were used at a 1:100 dilution. All antibodies were anti-mouse and their specificity was validated in previous studies performed in our laboratory[3,8,12,27–29].

MSC culture

$CD45^{-}Ter119^{-}CD31^{-}$ (TN) $Scf\text{-}GFP^{+}$ stromal cells from digested BM were seeded in α-MEM media (Gibco) supplemented with 20 % fetal bovine serum (FBS; Gibco), 100 units/ml of penicillin and 100μg/ml of streptomycin, 10ng/ml of fibroblast growth factor (FGF)-basic (R&D Systems) and 2mM of L-glutamine (Thermo Fisher Scientific) or CFU-F culture media[8] of phenol red–free α-MEM (Gibco) supplemented with 10 % FBS, 10 % MesenCult stimulatory supplement (STEMCELL Technologies), and 100 units/ml of penicillin and 100μg/ml of streptomycin. After 2–3 weeks of culture (passage 2–3), stromal cells were aliquoted and frozen with Recovery Cell Culture Freezing Medium (Gibco) and placed into liquid nitrogen. For control stroma, empty vector was infected into passage 2–3 stromal cells and cultured one passage prior to freezing into aliquots. For each experiment, we used these aliquots to minimize experimental variations.

Plasmid construction

For overexpression of *Atf4*, *Ctnnb1*, *Foxc1*, *Prrx1*, *Tsc22d1*, *Foxn3*, *Ostf1*, *Irf3* and *Irf7*, we amplified the coding regions of candidate genes by RT-PCR using Advantage HD Polymerase (Clontech) from pYX-Asc/*Atf4*, pYX-Asc/*Ctnnb1*, pYX-Asc/*Foxc1*, pYX-Asc/*Prrx1*, pYX-Asc/*Tsc22d1*, pSPORT1/*Foxn3* and pDNR-LIB/*Ostf1* vectors (provided by John F. Reidhaar-Olson at the Einstein shRNA Facility) or pCAGGS/*Irf3* and pCAGGS/*Irf7* vectors (a kind gift from T. Taniguchi, Univ. of Tokyo, Japan), then cloned these sequences into pENTR-D-TOPO (Thermo Fisher Scientific), confirmed the sequence of candidate genes by direct sequencing, and recombined the resulting plasmids with FUWC-GW vector which has Gateway and Ubiquitin C (UbC) promoter without markers (a kind gift from Chan-Jung Chang at Mount Sinai School of Medicine and Eric E. Bouhassira at Albert Einstein College of Medicine) by LR reaction of Gateway cloning System (Thermo Fisher Scientific). For overexpression of *Dlx5*, pENTR/*Dlx5* vector (purchased from DF/HCC DNA Resource Core at Harvard Medical School) was recombined with FUWC-GW vector by LR reaction of Gateway cloning System. For overexpression of *Fos*, *Hes6*, *Id1*, *Jun*, *Junb*, *Klf7*, *Nupr1*, *Pttg1*, *Snai2*, *Xbp1*, *Zfp36*, *HoxA9*, *Meis1*, *Stat3*, *Hes1*, *Myc*, *Stat5a* and *Runx2*, we recombined pCMV-SPORT6/gene vectors (Open Biosystems Library provided by John F. Reidhaar-Olson at the Einstein shRNA Facility) or pEF/*Runx2* vectors (a kind gift from S. Maeda, Univ. of Kagoshima, Japan) with pDONR221 vector (Thermo Fisher Scientific) by BP reaction of Gateway cloning System (Thermo Fisher Scientific). Then recombined the resulting plasmids with FUWC-GW vector by LR reaction of Gateway cloning System. All the vectors were confirmed to have the correct gene sequence by direct sequencing.

Lentivirus production

To selectively overexpress candidate genes in cultured stromal cells, lentiviruses were generated by transfecting 12μg of FUWC-GW/candidate gene vectors or empty control vector, and packaging vectors (0.6μg tat vector, 0.6μg rev vector, 0.6μg gag/pol vector, and 1μg vsv-g vector) into HEK-293T cells using 45μl TransIT-X2 transfection reagent (Mirus Bio). Supernatant was collected from transfected HEK-293T cells, filtrated with 0.45μm membrane (CORNING), and concentrated by ultracentrifugation.

Overexpression of candidate genes, isolation of single cell-derived clones and identification of virally integrated factors

Scf-GFP$^+$ stromal cells from BM were cultured for 3 weeks and transduced with a mix of concentrated lentivirus harbouring 28 genes. On day 5 post transduction, induced *Scf*-GFP$^+$ cells were sorted and limiting dilution was performed to isolate single cell-derived clones. To identify virally integrated factors in each clone, lentivirus-transduced stromal cells were collected and treated with nuclei lysis solution, incubated with RNase for 30 min at 37°C, and genomic DNA was purified with the Wizard Genomic DNA Purification Kit (Promega). Then PCR was performed with the resulting genomic DNA using a forward primer targeting the UbC promoter to discriminate the transgenes from the endogenous genes and reverse primers targeting an exon-exon junction of each candidate gene or designed to make PCR product around 350–450 base pairs (bp) in each candidate gene. The sequences of the

primers can be provided upon request. To overexpress *Klf7* alone in cultured stromal cells, a lentivirus harbouring pHIV-Tomato/*Klf7* was generated as described above. *Scf*-GFP$^+$ stromal cells were then transduced with concentrated lentivirus, and Tomato$^+$ cells were sorted on day 5 post-transduction. Control MSCs were similarly transduced with a control lentivirus containing an empty pHIV-Tomato vector.

Knockdown and overexpression of specific genes in rMSC

To selectively knockdown *Mef2c* in rMSC, lentiviruses of *Mef2c*/Control short hairpin RNA (shRNA) were generated by co-transfecting HEK-293T cells with 12μg shRNA shuttle vector (GIPZ Lentiviral shRNA Library, Open Biosystems, provided by Einstein shRNA Facility), 0.6 μg tat vector, 0.6 μg gag/pol vector, 1 μg vsv-g vector into HEK-293T cells using 45 μl TransIT-X2 transfection reagent (Mirus Bio). Supernatant was collected from HEK-293T cells, filtrated with 0.45 μm membrane (CORNING), and concentrated by ultracentrifugation. Concentrated virus preparations were used to transduce rMSC, and cells expressing the construct were selected by using 5.0μg/ml puromycin. To overexpress *Mef2c* in rMSC, lentiviruses were produced in HEK-293T cells as described above. rMSCs were transduced with concentrated lentiviral preparations, and Tomato$^+$ cells sorted on day 5 post-transduction.

In vitro mesensphere culture and differentiation assays

Mesensphere formation assays were done by plating empty vector-transduced control MSCs or rMSCs at clonal densities in 6-well plates (mesenspheres: 2000 cells/well) under culture conditions previously described[8]. Cells were cultured for 12–14 days upon which the spheres were scored. For mesensphere cultures, low adhesion tissue culture plates (STEMCELL Technologies) were used.

For osteogenic, adipogenic, and chondrogenic differentiation, control MSCs or rMSCs were treated with StemXVivo Osteogenic, Adipogenic, or Chondrogenic mouse differentiation media, according to the manufacturer's instructions (R&D Systems) as previously described[5,8]. All cultures were maintained with 5 % CO_2 in a water-jacketed incubator at 37°C. At specific time points, cells were collected for staining and RNA analysis.

Adipocytes were identified by the typical production of lipid droplets and were stained with Oil Red O as follows: cells were washed with 60 % isopropanol and allowed to dry completely. Oil Red working solution was prepared as a 6:4 dilution in bidistilled water of a 0.35g/ml Oil Red O solution in isopropanol (Sigma), and filtered 20 min later. Cells were incubated for 10 min with Oil red working solution and rinsed four times. Osteogenic differentiation indicated by mineralization of extracellular matrix and calcium deposits was revealed by Alizarin Red S staining. Cells were fixed with 4 % paraformaldehyde (PFA) for 30 min. After rinsing in distilled water, cells were stained with 40 mM Alizarin Red S (Sigma-Aldrich) solution at pH 4.2, rinsed in distilled water, and washed in Tris-buffered saline for 15 min to remove nonspecific staining. Chondrocytes were revealed by Alcian blue staining, which detects the synthesis of mucopolysaccharides. Cell pellets were incubated for 30 min at room temperature with 1% Alcian blue 8GX (Sigma) in 3 % acetic acid, pH 2.5, and rinsed four times.

Co-culture of murine Lin⁻ cells with murine MSCs

To assess expansion of phenotypic HSCs after co-culture with MSCs, $2x10^5$ Lin⁻ cells were isolated from C57BL/6-CD45.1/2 BM by MACS column (Miltenyi Biotec) depletion and co-cultured with MSCs for 6 days in StemSpan SFEM media (STEMCELL Technologies) supplemented with 10 % KnockOut Serum Replacement (Thermo Fisher Scientific), Pen/Strep, and cytokines. Cytokine concentrations were 20ng/ml of stem cell factor (SCF, PeproTech) and 10ng/ml of thrombopoietin (TPO; PROSPEC) unless otherwise noted. After co-culture for 6 days, HSC numbers were assessed by FACS analysis

BM transplantation after co-culture with rMSCs

Competitive repopulation assays were performed using the CD45.1/CD45.2 congenic system. CD45.2 recipient mice were lethally irradiated (12 Gy, two split doses) in a Cesium Mark I irradiator (JL Shepherd & Associates). For competitive repopulation assays, $2x10^5$ Lin⁻ cells were isolated from CD45.1 BM by MACS column (Miltenyi Biotec) depletion, co-cultured with rMSCs for 6 days in StemSpan SFEM media (STEMCELL Technologies) supplemented with 10 % KnockOut Serum Replacement (Thermo Fisher Scientific), Pen/Strep, 10ng/ml of TPO (PROSPEC). After co-culture for 6 days, $CD45^+$ cells were isolated with MACS column (Miltenyi Biotec) and were transplanted into lethally irradiated recipients together with $2x10^5$ of CD45.2 BM mononuclear cells (BMNCs). CD45.1/CD45.2 chimerism of recipient peripheral blood (PB) was analysed up to 4 months after transplantation by FACS analysis. For secondary BM transplantation, $1x10^6$ BMNCs from primary recipient chimeric mice were transplanted into irradiated CD45.2 recipients together with 1 x 10^6 of CD45.2 BMNCs.

For non-competitive repopulation assays to evaluate the ability to radio-protect lethally irradiated recipients, 25,000 or 40,000 non-cultured whole BMNCs (CD45.1) or expanded whole BMNCs (CD45.1), co-cultured with control MSCs, rMSCs or without stroma for 6 days in StemSpan SFEM media (STEMCELL Technologies) supplemented with 10 % KnockOut Serum Replacement (Thermo Fisher Scientific), Pen/Strep, 10ng/ml of TPO (PROSPEC) then collected and $CD45^+$ cells isolated by MACS column (Miltenyi Biotec), were transplanted into lethally irradiated (12 Gy, two split doses) CD45.2 recipients. Survival was analysed up to 2 months after transplantation.

Co-culture of human cord blood cells with murine rMSCs

CD34+ human cord blood (Lonza) was obtained according to an institutional review board-approved protocol. 13,600 $CD34^+$ cells were co-cultured with murine rMSCs in StemSpan SFEM media (STEMCELL Technologies) supplemented with 10 % KnockOut Serum Replacement (Thermo Fisher Scientific), Pen/Strep, 10ng/ml of human TPO (PROSPEC). After co-culture for 6 days, the number of phenotypic $Lin^-CD34^+CD38^-CD90^+CD49f^+$ human HSCs was assessed by FACS analysis.

Limiting dilution CRU assay of murine HSCs

Competitive repopulating unit (CRU) assays were performed as previously described[29] using limiting numbers of BMNCs from CD45.1 donor mice. Freshly isolated BMNCs were immediately used for BM transplantation, or BMNCs were co-cultured with rMSCs for 6

days in StemSpan SFEM media (STEMCELL Technologies) supplemented with 10 % KnockOut Serum Replacement (Thermo Fisher Scientific), Pen/Strep, 10ng/ml of TPO (PROSPEC) and 20ng/ml of stem cell factor (SCF; PEPROTEC), then collected and $CD45^+$ cells were isolated by MACS column (Miltenyi Biotec), and finally a fraction of the cultured cells corresponding to the indicated number (1,000, 2,500, 5,000, 12,500 and 25,000) of initial BMNCs was subjected to BM transplantation. The test cells (CD45.1) were transplanted together with 2 x 10^5 competitor BMNCs (CD45.2) into CD45.2 recipient mice lethally irradiated (12 Gy, two split doses). The percentage of donor ($CD45.1^+$) cells in the PB was determined 16 weeks later by flow cytometry. Mice with more than 1 % in all three lineages (myeloid, B and T cells) were considered positive and the others were defined as negative mice. The CRU frequency was calculated using L-Calc software (STEMCELL Technologies).

Limiting dilution CRU assay of human cord blood

CRU assays were performed using limiting numbers of $CD34^+$ cells from human cord blood (Lonza). Freshly isolated non-cultured human cord blood $CD34^+$ cells were immediately used for BM transplantation, or human cord blood $CD34^+$ cells were co-cultured with murine rMSCs for 6 days in StemSpan SFEM media (STEMCELL Technologies) supplemented with 10 % KnockOut Serum Replacement (Thermo Fisher Scientific), Pen/Strep, 10ng/ml of human TPO (PROSPEC) and 20ng/ml of human SCF (PROSPEC), then collected and human $CD45^+$ cells were isolated by MACS column (Miltenyi Biotec), and finally a fraction of the cultured cells corresponding to the indicated number (0.2, 1, 3 and 5 × 10^3) of initial cord blood cells was subjected to BM transplantation. The test cells (human $CD45^+$) were transplanted into *NOD-scid Il2rg*$^{-/-}$ (NSG) immunocompromised mice sublethally irradiated (2 Gy) together with 2 x 10^5 competitor BMNCs (NSG). The percentage of donor (human $CD45^+$) cells in the PB was determined 16 weeks later by flow cytometry. Mice with more than 1% were considered positive and the others were defined as negative mice. The CRU frequency was calculated using L-Calc software (STEMCELL Technologies).

Immunofluorescence staining and imaging of sorted HSCs

Immunofluorescence staining for γH2AX was adapted from previously described[16]. After co-culture in serum-free medium supplemented with SCF (20ng/ml) and TPO (10ng/ml) for 6 days, $Lin^-Sca\text{-}1^+c\text{-}Kit^+CD48^-CD150^+$ HSCs were directly sorted on polylysine-coated slides (P0425–72AE; Sigma), 500–2000 cells per slide, incubated for 10 min, fixed with 4 % PFA for 10 min at room temperature, and permeabilised with 0.2 % Triton X-100 for 20 min at room temperature. Subsequently, the cells were blocked with 1% BSA/PBS overnight at 4 °C. Cells were then incubated with 0.125 μg (5μl of 25μg/ml) FITC-conjugated anti-phospho-H2A.X (Ser139) antibody (Clone: 2F3; Cat: 613404; BioLegend) for 2 h at 37°C. Primary antibody staining was followed by 3 washes with PBS and 10 min incubation with 0.2 % Hoechst 33342 (Sigma). All images were acquired using ZEISS AXIO examiner D1 microscope (Zeiss) with confocal scanner unit (Yokogawa), and reconstructed in three dimensions with Slide Book software (Intelligent Imaging Innovations). Image analysis was performed using the Slide Book software (Intelligent Imaging Innovations).

RNA isolation and real-time quantitative PCR (qPCR)

RNA isolation and qPCR were performed as described previously[12]. mRNA expression levels were calculated relative to *Gapdh* or *Actinb* (*β-Actin*). The sequences of the primers are provided in Supplementary Table 5.

RNA-seq and analysis

Total RNA from 1,000–5,000 sorted MSCs was extracted using the RNeasy Plus Micro kit (QIAGEN), and assessed for integrity and purity using an Agilent 2100 Bioanalyzer (Agilent Technologies). Complementary DNA libraries were then generated using the SMART-Seq v4 Ultra Low Input RNA Kit for Sequencing (Clontech) and the Nextera XT DNA Sample preparation Kit (Illumina). The libraries were then submitted for Illumina NextSeq 500 sequencing (150 bp single ended) according to the standard procedures (ENSEMBL Mus musculus reference genome GRCm38 release 77). RNA-seq data output from the Illumina NextSeq 500 platform were processed as previously described[3,30]. Briefly, single- and paired-ended sequencing reads were aligned to the mouse genome (mm10) using Spliced Transcripts Alignment to a Reference (STAR 2.4.1c)[31]. Aligned reads were then quantified to the transcriptome (UCSC mm10 annotation) at the gene level using featureCounts (v1.4.6)[32]. Read counts were then normalized to reads per kilobase per million (RPKM) and differentially expressed genes were identified using the Characteristic Direction method[33]. Principal Component Analysis (PCA) and pathway analysis with Enrichr[34,35] were then performed. Quality Control summary is shown in Supplementary Table 3.

ATAC-seq and analysis

ATAC-seq was performed as previously described[36,37]. 2,700–5,000 MSCs were sorted into 4°C 1× PBS and washed in cold 1× PBS, lysed using cold lysis buffer (10 mM Tris-HCl, pH 7.4, 10 mM NaCl, 3 mM $MgCl_2$ and 0.1% Igepal CA-630) to obtain nuclei. Immediately after lysis, nuclei were spun at 500 g for 10 min using a refrigerated centrifuge. To perform Transpose reaction, immediately following the nuclei prep, the nuclei pellet was resuspended in the transposase reaction mix (2.5 μl 2× TD buffer, 0.25 μl transposase (Illumina) and 2.25 μl nuclease-free water). The transposition reaction was carried out for 30 min at 37 °C. We then amplified the library fragments using 5 μl of transposed DNA, 10 μl of nuclease-free H_20, 25 μl of NEBnext High-Fidelity 2× PCR master mix (New England Biolabs), 2.5 μl of 25 μM custom PCR primers 1, and 2.5 μl of 25 μM Barcode PCR primers 2 (primer sequences are previously described[37]), using the following PCR conditions: 72°C for 5 min; 98°C for 30 s; and thermocycling at 98°C for 10 s, 63°C for 30 s and 72°C for 1 min. We amplified the libraries for a total of 13 or 17 cycles. The appropriate number of cycles for PCR amplification was determined through qPCR as described[34]. After the initial 5 cycles additional 8 or 12 cycles were performed depending on the yield measured by qPCR. All libraries were sequenced on the Illumina Hiseq 2500 with 100 bp paired-end reads. We performed analysis on three biological replicates.

The obtained sequences were adapter trimmed and aligned to the mouse reference genome (mm10 including small contigs) using the *BWA-MEM* software (arXiv:1303.3997v1). We selected and used only uniquely aligned reads for the analysis. Reads aligned to mitochondrial DNA and PCR duplicate reads were eliminated from further analysis. Read

numbers were down-sampled so that peak calling was based on comparable numbers of reads for each sample. We performed peak calling using *MACS2*[38] and calculated the irreproducible discovery rates (IDR)[39] of the detected peaks between biological replicates to select the high confidence peaks (IDR < 0.05). We selected peaks which were shared across at least two biological replicates with an IDR <0.05. The overlap of peaks was then compared between samples, and pathway analysis was performed with Enrichr[34,35] For motif analysis, loci where chromatin changed between samples from open to closed or the opposite pattern were identified. The sequences at these loci were analysed for transcription factor binding sites using *HOMER*[40]. Quality Control summary is shown in Supplementary Table 4.

Statistics & Reproducibility

All data are represented as mean±s.d., except for qPCR that are represented as mean±s.e.m, unless otherwise noted in the figure legends. Comparisons between two samples were done using unpaired two-tailed Student's *t* tests. Comparison between multiple groups was performed using one-way ANOVA followed by Tukey's multiple comparison test. Log-rank analyses were used for Kaplan-Meier survival curves. All data presentation and statistical analyses were performed using GraphPad Prism7 (GraphPad Software, San Diego, CA). **P* < 0.05, ***P* < 0.01, ****P* < 0.001, *****P* < 0.0001, n.s. (not significant). *P* values > 0.001 are given in figure legends.

All experiments were reproduced at least three times, except for those of Fig. 3j and Supplementary Fig. 1l–m which were reproduced twice.

Supplementary Material

Refer to Web version on PubMed Central for supplementary material.

Acknowledgements

We thank Colette Prophete and Paul Ciero for technical assistance, Dr. Lydia Tesfa for assistance with cell sorting and Dr. Shahina Maqbool for RNA sequencing. We thank Drs. Lei Ding and Sean J. Morrison for providing the *Scf*-GFP knock-in mice. We thank Drs. Chan-Jung Chang and Eric E. Bouhassira for the FUWC-GW and pHIV-dTmt vectors. We thank Dr. Tadatsugu Taniguchi (Univ. of Tokyo, Japan) for the pCAGGS/*Irf3* and pCAGGS/*Irf7* vectors and Dr. Shingo Maeda (Univ. of Kagoshima, Japan) for the pEF/Runx2 vectors. We thank Drs. John F. Reidhaar-Olson and Jidong Shan for supplying overexpression and knockdown vectors. This work was supported by R01 grants from the National Institutes of Health (NIH) (DK056638, HL069438, DK116312, DK112976 to P.S.F., and U54HL127624, U24CA224260 to A.M.). We are also grateful to the New York State Department of Health (NYSTEM Program) for shared facility (C029154) and research support (N13G-262) and the Leukemia and Lymphoma Society's Translational Research Program. F.N. was supported by the Postdoctoral Fellowship for Research Abroad from the Japan Society for the Promotion of Science (JSPS). D.K.B. is partially supported by a NIH Training Grant (T32 GM007288). M.M. is a New York Stem Cell Foundation (NYSCF) Druckenmiller fellow. A.H.Z was supported by a NIH Training Grant (T32 NS007098) and by a National Cancer Institute (NCI) predoctoral M.D./Ph.D. fellowship (F30 CA203446). P.E.B is supported by a postdoctoral fellowship from Fonds de recherche du Québec-Santé (FRQS).

References:

1. Pinho S & Frenette PS Haematopoietic stem cell activity and interactions with the niche. Nat Rev Mol Cell Biol (2019).
2. Morrison SJ & Scadden DT The bone marrow niche for haematopoietic stem cells. Nature 505, 327–334 (2014). [PubMed: 24429631]

3. Asada N et al. Differential cytokine contributions of perivascular haematopoietic stem cell niches. Nat Cell Biol 19, 214–223 (2017). [PubMed: 28218906]
4. Khan JA et al. Fetal liver hematopoietic stem cell niches associate with portal vessels. Science (New York, N.Y.) 351, 176–180 (2016).
5. Mendez-Ferrer S et al. Mesenchymal and haematopoietic stem cells form a unique bone marrow niche. Nature 466, 829–834 (2010). [PubMed: 20703299]
6. Butler JM et al. Endothelial cells are essential for the self-renewal and repopulation of Notch-dependent hematopoietic stem cells. Cell Stem Cell 6, 251–264 (2010). [PubMed: 20207228]
7. Isern J et al. Self-renewing human bone marrow mesenspheres promote hematopoietic stem cell expansion. Cell Rep 3, 1714–1724 (2013). [PubMed: 23623496]
8. Pinho S et al. PDGFRalpha and CD51 mark human nestin+ sphere-forming mesenchymal stem cells capable of hematopoietic progenitor cell expansion. J Exp Med 210, 1351–1367 (2013). [PubMed: 23776077]
9. Otto F et al. Cbfa1, a candidate gene for cleidocranial dysplasia syndrome, is essential for osteoblast differentiation and bone development. Cell 89, 765–771 (1997). [PubMed: 9182764]
10. Oguro H et al. Differential impact of Ink4a and Arf on hematopoietic stem cells and their bone marrow microenvironment in Bmi1-deficient mice. The Journal of Experimental Medicine 203, 2247–2253 (2006). [PubMed: 16954369]
11. Omatsu Y, Seike M, Sugiyama T, Kume T & Nagasawa T Foxc1 is a critical regulator of haematopoietic stem/progenitor cell niche formation. Nature 508, 536–540 (2014). [PubMed: 24590069]
12. Kunisaki Y et al. Arteriolar niches maintain haematopoietic stem cell quiescence. Nature 502, 637–643 (2013). [PubMed: 24107994]
13. Ding L, Saunders TL, Enikolopov G & Morrison SJ Endothelial and perivascular cells maintain haematopoietic stem cells. Nature 481, 457–462 (2012). [PubMed: 22281595]
14. Wei Q & Frenette PS Niches for Hematopoietic Stem Cells and Their Progeny. Immunity 48, 632–648 (2018). [PubMed: 29669248]
15. Itoh K et al. Reproducible establishment of hemopoietic supportive stromal cell lines from murine bone marrow. Exp Hematol 17, 145–153 (1989). [PubMed: 2783573]
16. Flach J et al. Replication stress is a potent driver of functional decline in ageing haematopoietic stem cells. Nature 512, 198–202 (2014). [PubMed: 25079315]
17. Beerman I, Seita J, Inlay MA, Weissman IL & Rossi DJ Quiescent hematopoietic stem cells accumulate DNA damage during aging that is repaired upon entry into cell cycle. Cell Stem Cell 15, 37–50 (2014). [PubMed: 24813857]
18. Rube CE et al. Accumulation of DNA damage in hematopoietic stem and progenitor cells during human aging. PLoS One 6, e17487 (2011). [PubMed: 21408175]
19. Rossi DJ et al. Deficiencies in DNA damage repair limit the function of haematopoietic stem cells with age. Nature 447, 725–729 (2007). [PubMed: 17554309]
20. Walter D et al. Exit from dormancy provokes DNA-damage-induced attrition in haematopoietic stem cells. Nature 520, 549–552 (2015). [PubMed: 25707806]
21. Yamazaki S et al. Nonmyelinating Schwann cells maintain hematopoietic stem cell hibernation in the bone marrow niche. Cell 147, 1146–1158 (2011). [PubMed: 22118468]
22. Torisawa YS et al. Bone marrow-on-a-chip replicates hematopoietic niche physiology in vitro. Nat Methods 11, 663–669 (2014). [PubMed: 24793454]
23. Dhami SP, Kappala SS, Thompson A & Szegezdi E Three-dimensional ex vivo co-culture models of the leukaemic bone marrow niche for functional drug testing. Drug Discov Today 21, 1464–1471 (2016). [PubMed: 27130156]
24. Naldini L Gene therapy returns to centre stage. Nature 526, 351–360 (2015). [PubMed: 26469046]
25. Kawamura Y, Tanaka Y, Kawamori R & Maeda S Overexpression of Kruppel-like factor 7 regulates adipocytokine gene expressions in human adipocytes and inhibits glucose-induced insulin secretion in pancreatic beta-cell line. Mol Endocrinol 20, 844–856 (2006). [PubMed: 16339272]

26. Xu G et al. Expression of XBP1s in bone marrow stromal cells is critical for myeloma cell growth and osteoclast formation. Blood 119, 4205–4214 (2012). [PubMed: 22427205]
27. Pierce H et al. Cholinergic Signals from the CNS Regulate G-CSF-Mediated HSC Mobilization from Bone Marrow via a Glucocorticoid Signaling Relay. Cell Stem Cell 20, 648–658 e644 (2017). [PubMed: 28196601]
28. Bruns I et al. Megakaryocytes regulate hematopoietic stem cell quiescence through CXCL4 secretion. Nat Med 20, 1315–1320 (2014). [PubMed: 25326802]
29. Lucas D et al. Chemotherapy-induced bone marrow nerve injury impairs hematopoietic regeneration. Nat Med 19, 695–703 (2013). [PubMed: 23644514]
30. Wang Z & Ma'ayan A An open RNA-Seq data analysis pipeline tutorial with an example of reprocessing data from a recent Zika virus study [version 1; referees: 3 approved]. F1000Research 5 (2016).
31. Dobin A et al. STAR: ultrafast universal RNA-seq aligner. Bioinformatics 29, 15–21 (2013). [PubMed: 23104886]
32. Liao Y, Smyth GK & Shi W featureCounts: an efficient general purpose program for assigning sequence reads to genomic features. Bioinformatics 30, 923–930 (2014). [PubMed: 24227677]
33. Clark N et al. The characteristic direction: a geometrical approach to identify differentially expressed genes. BMC Bioinformatics 15, 79 (2014). [PubMed: 24650281]
34. Kuleshov MV et al. Enrichr: a comprehensive gene set enrichment analysis web server 2016 update. Nucleic Acids Res 44, W90–97 (2016). [PubMed: 27141961]
35. Chen EY et al. Enrichr: interactive and collaborative HTML5 gene list enrichment analysis tool. BMC Bioinformatics 14, 128 (2013). [PubMed: 23586463]
36. Buenrostro JD, Wu B, Chang HY & Greenleaf WJ ATAC-seq: A Method for Assaying Chromatin Accessibility Genome-Wide. Curr Protoc Mol Biol 109, 21 29 21–29 (2015).
37. Buenrostro JD, Giresi PG, Zaba LC, Chang HY & Greenleaf WJ Transposition of native chromatin for fast and sensitive epigenomic profiling of open chromatin, DNA-binding proteins and nucleosome position. Nat Methods 10, 1213–1218 (2013). [PubMed: 24097267]
38. Zhang Y et al. Model-based analysis of ChIP-Seq (MACS). Genome Biol 9, R137 (2008). [PubMed: 18798982]
39. Li Q, Brown JB, Huang H & Bickel PJ Measuring reproducibility of high-throughput experiments. The Annals of Applied Statistics 5, 1752–1779 (2011).
40. Heinz S et al. Simple combinations of lineage-determining transcription factors prime cis-regulatory elements required for macrophage and B cell identities. Mol Cell 38, 576–589 (2010). [PubMed: 20513432]

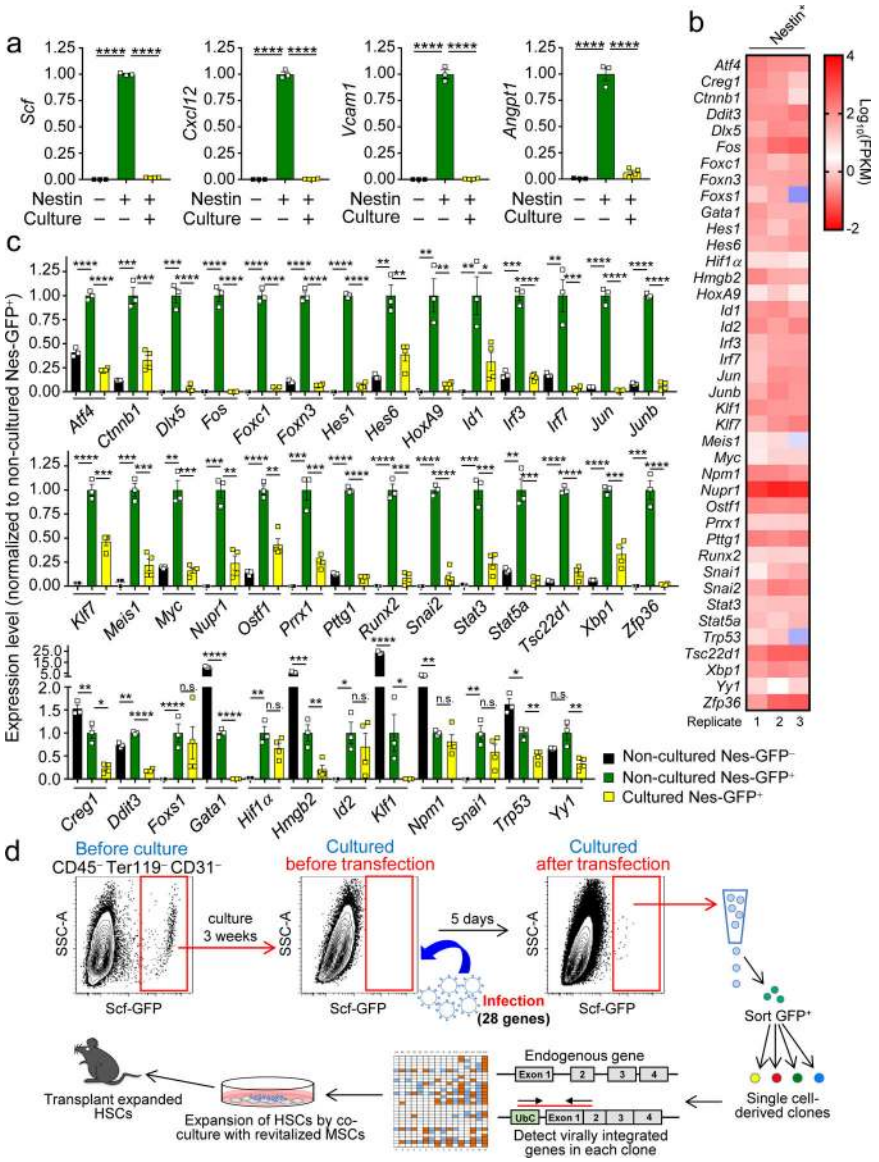

Figure 1. Selection and screening of candidate genes for revitalizing MSCs.

(**a**) Real-time qPCR analysis of the expression of *Scf, Cxcl12, Angpt1* and *Vcam1* in freshly isolated Nestin-GFP^{-} and Nestin-GFP^{+} CD45^{-}Ter119^{-}CD31^{-} cells and 2 weeks *in vitro* cultured Nestin-GFP^{+} cells isolated from *Nes-Gfp* transgenic mice. Expression level was normalized with *Gapdh* level and the mean expression level in freshly isolated Nestin-GFP^{+} was defined as 1. n=3 biologically independent samples for Nestin-GFP^{-}, Nestin-GFP^{+} mice; n=4 biologically independent samples for cultured-Nestin-GFP^{+}. (**b**) Selected 40 candidate genes tested for revitalizing cultured MSCs were derived from RNA-seq analyses of Nestin-GFP^{+} CD45^{-}Ter119^{-}CD31^{-} cells[12]. Levels of expression (FPKM) are shown. n=3 biologically independent samples. (**c**) Real-time qPCR analysis of the expression of 40 candidate genes in freshly isolated Nestin-GFP^{-} cells, freshly isolated Nestin-GFP^{+} MSCs, and 2 weeks *in vitro* cultured Nestin-GFP^{+} MSCs. Expression level was normalized with *Gapdh* level and the mean expression level in freshly isolated Nestin-GFP^{+} was defined as 1.

n=3 biologically independent samples for Nestin-GFP^{-}, Nestin-GFP^{+}; n=4 biologically independent samples for cultured-Nestin-GFP^{+}. (**d**) Outline of experiment strategy in reprogramming cultured MSCs into revitalized MSCs. FACs plots are representative of five separate experiments. Error bars, mean±s.e.m. *P<0.05, **P<0.01, ***P<0.001, ****P<0.0001, n.s. (not significant); two-sided unpaired Student's t test (**a** and **c**). Refer to Supplementary Table 6 for precise P-values.

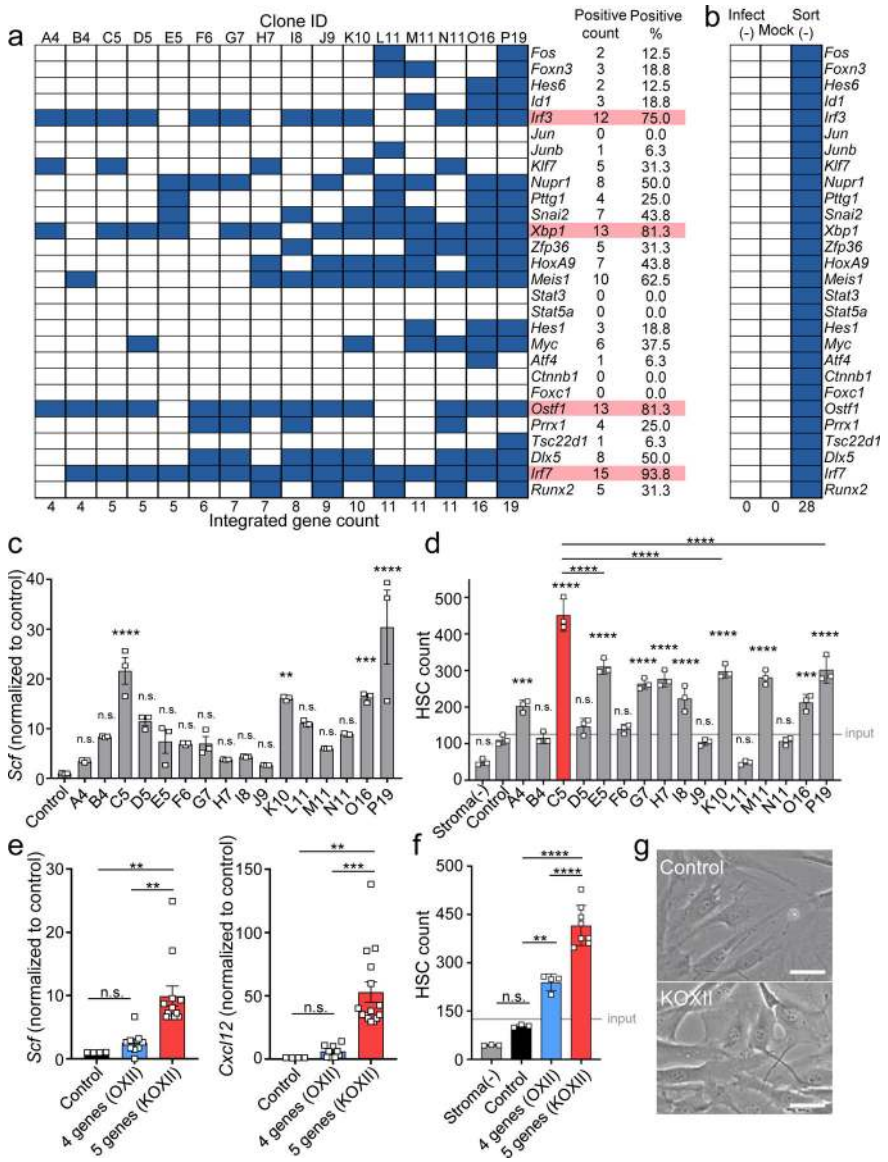

Figure 2. Combination of *Klf7, Ostf1, Xbp1, Irf3* and *Irf7* reprograms cultured MSCs and enables the *ex vivo* HSC maintenance and expansion.

(**a**) Presence (blue) or absence (white) of the indicated genes in each clone derived from *Scf*-GFP^{+} MSCs transduced with a mix of lentivirus harbouring 28 genes. Genes integrated in >75% of clones are highlighted in red. (**b**) Presence (blue) or absence (white) of virally integrated genes in cultured MSCs before transduction (Infect^{-}), transduced with empty vector (Mock), or transduced with mix of lentivirus harbouring 28 genes without sorting *Scf*-GFP^{+} cells (Sort^{-}). (**c**) *Scf* expression as determined by real-time qPCR analysis. Statistical significance indicates comparison to empty vector-transduced control MSCs. Mean expression in control MSC was defined as 1. n=3 biologically independent samples for each clone. K10, $P = 0.001$. (**d**) HSC numbers were assessed by FACS analysis after Lin^{-} BM cells were co-cultured with each single cell clone. Statistical significance indicates comparison to control. Horizontal line indicates the input HSC numbers. All 'n' represent biologically independent samples. n=3. (**e**) Expression of *Scf* and *Cxcl12* was assessed by

real-time qPCR in control MSC, OXII-transduced MSC clones (OXII), and KOXII-transduced MSC clones (KOXII). Mean expression level in control MSC was defined as 1. n=4 (Control), n=9 (OXII), n=12 (KOXII) for *Scf*. n=4 (Control), n=9 (OXII), n=15 (KOXII) for *Cxcl12*. KOXII vs. control, $P = 0.003$; vs. OXII, $P = 0.001$ for *Scf*. KOXII vs. control, $P = 0.002$ for *Cxcl12*. (**f**) Lin^- BM cells were co-cultured with control MSC, OXII-transduced MSC clones (OXII), and KOXII-transduced MSC clones (KOXII), and HSC numbers were assessed by FACS analysis. n=3 (Control), n=4 (OXII), n=8 (KOXII). OXII vs. control, $P = 0.006$. Data points in (d), (**e**), and (**f**) represent distinct single cell-derived clones. (**g**) Phase-contrast images of MSCs transduced with empty vector (control) and KOXII-transduced MSCs (KOXII) (scale bar represents 50μm). All 8 KOXII-transduced clones evaluated exhibited similar morphology. Error bars, mean±s.e.m. in (**c** and **e**), mean±s.d. in (**d** and **f**). $*P<0.05$, $**P<0.01$, $***P<0.001$, $****P<0.0001$, n.s. (not significant); One-way ANOVA followed by Tukey's multiple comparison test (**c-f**).

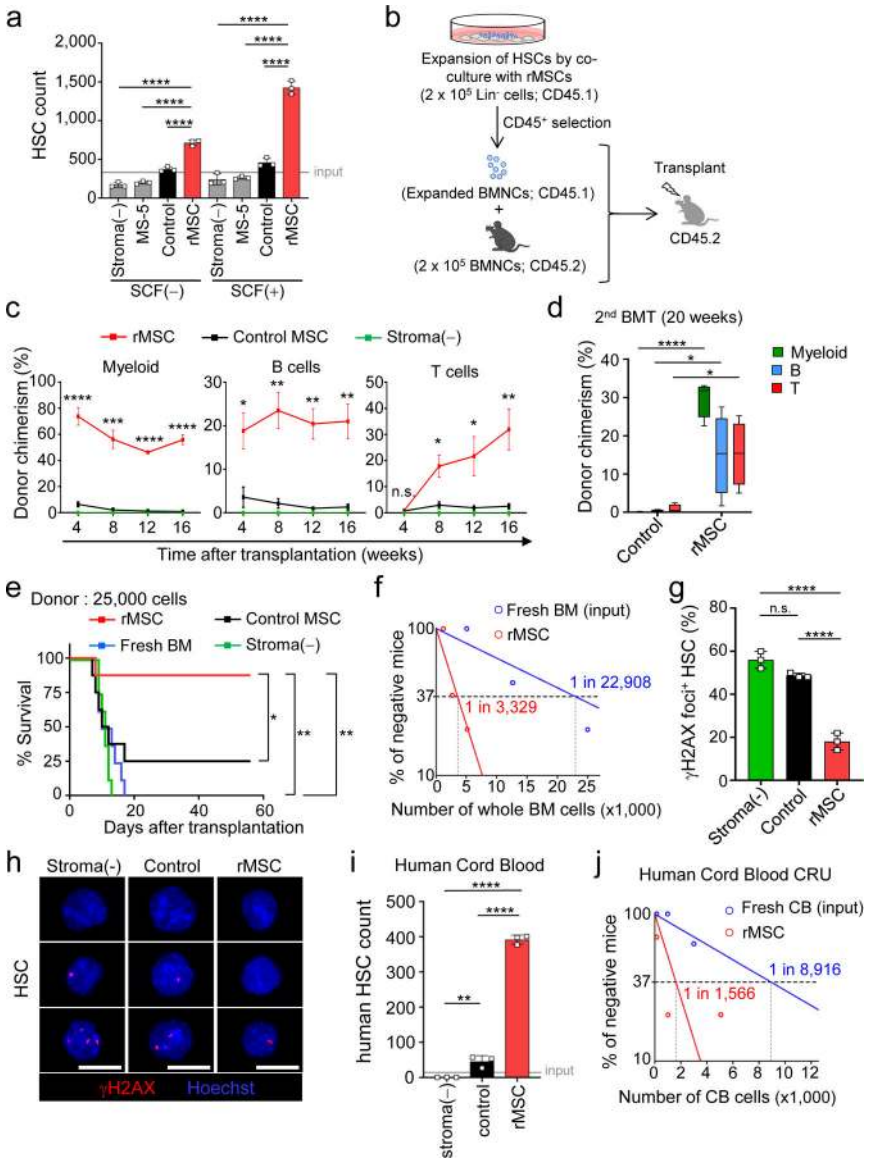

Figure 3. rMSCs maintain engraftable HSCs.

(**a**) Lin⁻ BM cells were co-cultured with MS-5, empty vector-transduced MSC (control), rMSC, or in cell-free media, with or without SCF (20 ng/ml), and HSC numbers were assessed by FACS. n=3 independent samples for MS-5, Control, and rMSC. (**b**) Experimental design of the competitive reconstitution assay. (**c**) Quantification of myeloid, B, and T cell engraftment by FACS in the blood of mice transplanted with Lin⁻ BM cells co-cultured with control MSCs, rMSCs, or cell-free media, by competitive reconstitution assay. Statistical significance was determined by comparing donor chimerism to control MSC. *P*-values are available in Supplementary Table 6. n=4 mice/group. (**d**) Long-term engraftment of myeloid, B (*P*=0.03), and T (*P*=0.01) cells in a secondary competitive reconstitution assay from the primary transplantation shown in (c). Box plots show median, first and third quartile, minimum and maximum. n=4 mice/group. (**e**) Kaplan-Meier survival curve of lethally irradiated recipient mice (CD45.2) non-competitively transplanted with 25,000 fresh

CD45.1 BMNCs (Fresh BM, P=0.001), or with CD45$^+$ cells from co-culture of 25,000 CD45.1 BMNCs with control MSCs (P=0.02), rMSCs, or cell-free media (P=0.001). n=8 mice/group. (**f**) Competitive-repopulating unit (CRU) assay using limiting numbers of fresh BMNCs, or BMNCs co-cultured with rMSCs. n=4 mice for rMSCs (1×10^3) and fresh BM ($2.5, 12.5\times10^3$); n=5 mice for rMSCs ($2.5, 5, 12.5, 25\times10^3$) and fresh BM ($5, 25\times10^3$). (**g** and **h**) Quantification (**g**) and representative images (**h**) of γH2AX (red) in HSCs. Nuclei were stained with Hoechst (blue). n was calculated as mean of 150 HSCs scored from n=3 biologically independent samples for each group. (**i**) 13,600 CD34$^+$ human CB cells were co-cultured and HSC numbers were assessed by FACS analysis. n=3 biologically independent samples for Control and rMSC. (**j**) CRU assay using limiting numbers of fresh CB CD34$^+$ cells or CD34$^+$ cells co-cultured with murine rMSCs. n=5 mice for each group. Scale bars: (**h**) 10μm. Error bars, mean±s.d. in (**a**, **g** and **i**), mean±s.e.m. in (**c**). *P<0.05, **P<0.01, ***P<0.001, ****P<0.0001; One-way ANOVA followed by Tukey's multiple comparison test (**a**, **g** and **i**), two-sided unpaired Student's t test (**c** and **d**), two-sided log-rank test (**e**).

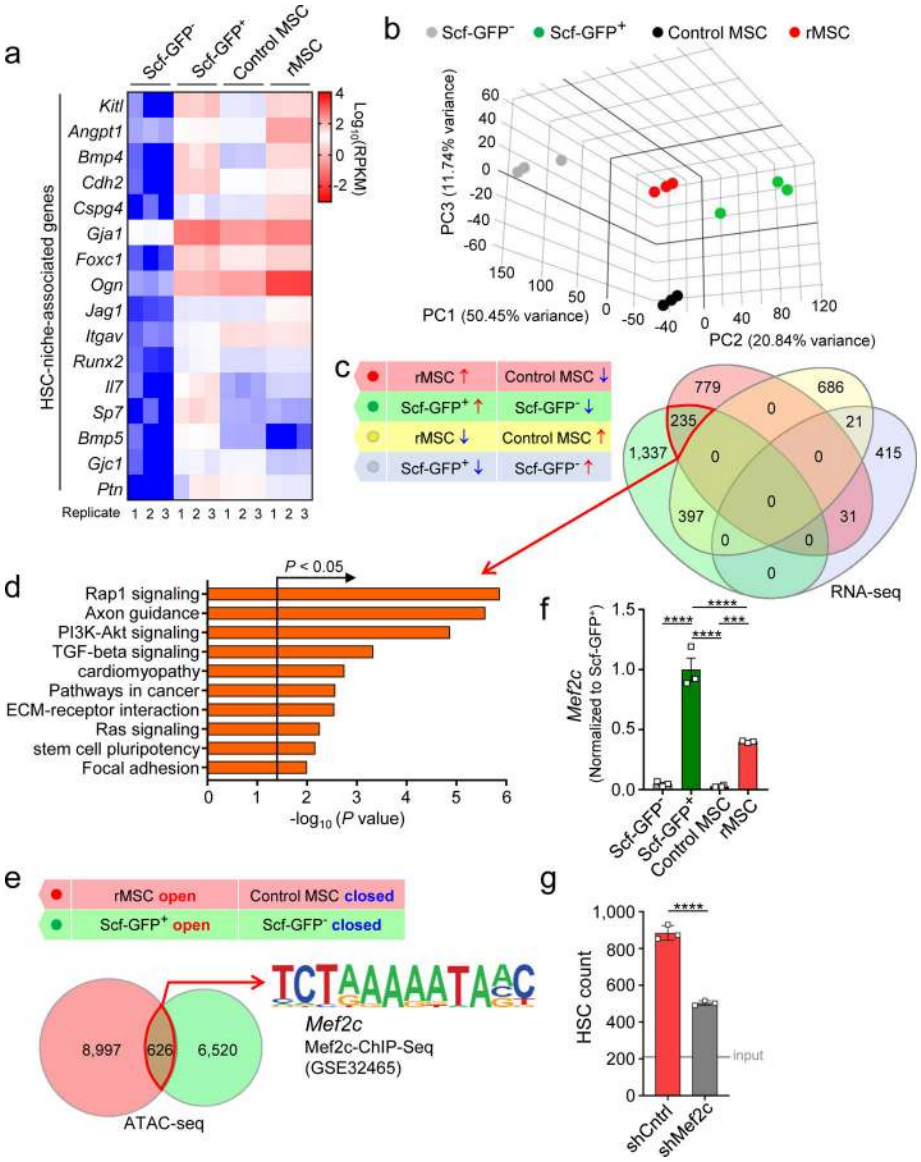

Figure 4. Characterization of rMSCs and *Mef2c* is one of key factors in revitalization of MSCs.

(**a**) Heat map of niche gene expression levels[3]. Expression levels in sorted non-cultured *Scf*-GFP⁻ CD45⁻Ter119⁻CD31⁻ cells, non-cultured *Scf*-GFP⁺ CD45⁻Ter119⁻CD31⁻ cells, empty vector-transduced control MSCs, and rMSCs. The values of log-transformed reads per kilobase per million mapped reads (RPKM) obtained from RNA-seq were visualized using GraphPad Prism7. Genes with absent expression were assigned to the lowest value of the gene pool for visualization. n=3 biologically independent samples for each group. (**b**) Principal Component Analysis (PCA) visualizes the samples from the four cell populations in the gene expression space obtained by RNA-seq profiling. n=3 biologically independent samples for each group. (**c**) Venn diagrams showing the overlap between the 4 groups of up and down regulated genes. (**d**) Enriched pathways for the 235 genes overlapping between the two groups in (c). Pathway enrichment analysis results from Enrichr[34,35]. *P*-values determined by one-sided Fisher's exact test for 230 pathways, with no correction for

multiple comparisons. (**e**) Venn diagrams to show the overlap between 2 groups of peaks with increased accessibilities (open) and peaks with decreased accessibilities (closed) in ATAC-seq analysis of the four cell populations. One of the top significant transcription regulators identified from motifs analysis of the 626 overlapping peaks is shown (*Mef2c*, $P = 1\times10^{-15}$). (**f**) Expression of *Mef2c* was assessed by real-time qPCR in the samples from the four cell populations. Expression level was normalized with *β-Actin* and the mean expression level in *Scf*-GFP^{+} cells was defined as 1. n=3 *Scf*-GFP^{-}, n=3 *Scf*-GFP^{+}, n=3 Control MSC, n=4 rMSC (n represents biologically independent samples). (**g**) Lin^{-} BM cells were co-cultured with shCntrl-transduced rMSCs and shMef2c-transduced rMSCs in the presence of SCF (20ng/ml) and TPO (10ng/ml). After 6 days, HSC numbers were assessed by FACS analysis. n=3 biologically independent samples for shCntrl and shMef2c. Error bars, mean±s.e.m. in (**f**), mean±s.d. in (**g**). *P<0.05, **P<0.01, ***P<0.001, ****P<0.0001; One-way ANOVA followed by Tukey's multiple comparison test (**f**), two-sided unpaired Student's *t* test (**g**).